Three-Dimensional Turbulence Analyses Using Turbulence Diagnostic Simulator

N. Kasuya, M. Yagi [a,b], K. Itoh and S.-I. Itoh [a]

National Institute for Fusion Science, 322-6 Oroshi-cho, Toki 509-5292, Japan

[a] *Research Institute for Applied Mechanics, Kyushu University, Kasuga, Fukuoka 816-8580, Japan*

[b] *Japan Atomic Energy Agency, 801-1 Mukoyama, Naka, Ibaraki 311-0193, Japan*

1. Introduction

Turbulence in toroidal plasmas forms meso-scale structures, such as a zonal flow and streamer, and it is important to clarify the role of the turbulence structures on anomalous transport [1]. High resolution measurements of fluctuations have been carried out in experimental devices to make quantitative estimation of turbulent transport [2]. Numerical simulations can give three-dimensional (3-D) turbulent fields, which represent fundamental phenomena in plasmas, so the simulation data are suitable as a test field to carry out detailed analyses for comparison with experimental results [3]. We have been developing a turbulence diagnostic simulator (TDS), which is the combination of fluid turbulence codes and numerical diagnostic modules to simulate experimental measurements of plasma turbulence [4]. In this paper, numerical diagnostics in a helical plasma are carried out using the TDS.

2. Turbulence Diagnostic Simulator

For turbulence analyses, we have been developing an assembly of codes, which consists of two main parts; turbulence codes and modules simulating experimental diagnostics. Turbulent fields are produced by fluid simulations using a supercomputer. Calculations in several kinds of magnetic configurations are carried out, and time series data of 3-D fluctuation fields are obtained. A large number of temporal points, which are sufficient for statistical analyses, are stored, so the data size is the order of tera-bytes in the case of toroidal plasmas. The stored data are analyzed using modules to simulate experimental diagnostics of turbulence, such as Beam Emission Spectroscopy (BES) and Heavy Ion Beam Probe (HIBP). The TDS includes the several turbulence codes and the several numerical measurement modules. The combination is selected in accordance with the research object.

3. Turbulence Simulation

Data analyses for a helical plasma are described in this paper. To provide turbulence data, the simulation code has been extended to calculate the drift-interchange turbulence in helical plasmas with a circular cross-section. The averaging method with the stellarator expansion [5] is applied to give a set of model equations for stream function u, ζ component of the vector potential A and total pressure P, as described in [6].

The nonlinear simulation is performed, using the following parameters: magnetic field B = 2.0 [T], electron temperature T_e = 1 [keV], minor radius a = 0.6 [m], major radius R_0 = 3.75 [m], viscosities $\mu = \eta = \eta_\perp = 1 \times 10^{-4}$, pole number l = 2, pitch number M = 10. Rotational transform ι is given by a monotonically increasing function with the radius from $\iota(0) = 0.31$ to $\iota(a) = 0.88$, so rational surfaces with m / n = 2 / 1 and 3 / 2 are included, but 1 / 1 is not in the plasma, where m and n are the poloidal and toroidal mode number, respectively. 1024 grids in the radial direction and Fourier modes $-32 \le m \le 32$, $-8 \le n \le 8$ are taken.

Spatio-temporal data of turbulent fields are generated by this global simulation. The calculation with a fixed pressure source, which forms a pressure profile peaked at r = 0, is carried out. Figure 1 (a) shows the time evolutions of the fluctuating energy of the electrostatic potential. Low m, n modes whose rational surfaces exist in the plasma are excited in the linear growing phase, and saturation is obtained with energy exchange between various modes by nonlinear couplings. The snapshots of the contours of the fluctuations are shown in Fig. 1 (b) and (c). In the saturated state, mode structures of low m, n modes, such as (m, n) = (1, 1) and (2, 1), spread broadly in the radial direction, and those of medium m, n modes, such as (3, 2) and (8, 4), are localized near their rational surfaces. Here, we assume that variables u and P represent the normalized electrostatic potential and density, respectively.

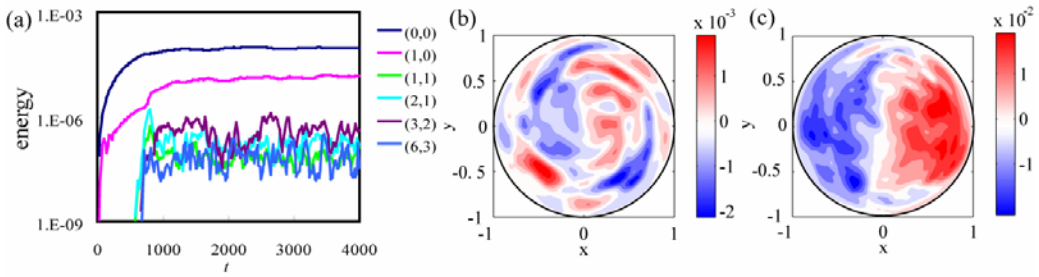

Fig. 1 (a) Time evolutions of the electrostatic potential energy of Fourier modes, and snapshots of (b) the electrostatic potential and (c) pressure fluctuations on the poloidal cross-section at t = 3000.

4. Numerical Diagnostic

Numerical diagnostics are carried out on simulation data as obtained in the previous section. Several modules are available for simulation of experimental diagnostics in the TDS. The examples to show the characteristic features of fluctuations are introduced in this section.

4.1. mean component generation

In our model, the mean flow is generated by the toroidal coupling with the mean pressure profile. In addition, turbulence perturbs the mean with nonlinear couplings. Here, we analyze the relationship between the turbulence and turbulence induced components. In experiments, a finite number of local observations give the radial profile. 1-D signals at $\theta = 0$ and $\zeta = 0$ are taken from 3-D fields to show the radial profile. Figure 2 (a) shows the time evolutions of the pressure fluctuations including all modes without the (0,0) mode in the simulation ($\tilde{P}_{m\neq 0}$) and

the (0,0) mode only ($\tilde{P}_{00}$). There exist localized modes in $r / a > 0.8$ as in the evolution of $\tilde{P}_{m\neq0}$, and the (3,2) mode has the largest amplitude, whose resonant surface is placed at $r / a \sim 0.83$. On the other hand, the perturbation of the (0,0) mode mainly exists in $r / a = 0.4$ - 0.7, and its temporal variation is rather slower, whose typical oscillation period is 400, compared with the oscillation period of the (3,2) mode ~ 60. Correlation between the turbulence ($\tilde{P}_{m\neq0}$) and the (0,0) mode ($\tilde{P}_{00}$) is calculated to estimate their relation. The 2-D profile of the correlation with the (0,0) mode at $r / a = 0.5$ is shown in Fig. 2 (b). The turbulence in $r / a = 0.4$ - 0.6 and $\theta = -\pi / 6$ - $\pi / 4$ (low field side) is strongly correlated with the (0,0) mode, though the perturbations in the region where the localized modes exist have no correlation. In this way, it is found that there is a region where the turbulence and the (0,0) mode are coupled with each other. In addition, the (0,0) mode is broad in the radial direction, and a two-time, two-point correlation analysis shows that the change in the region where the (0,0) mode exists propagates faster than those in the other regions. This is one of the candidates to cause the non-local transport observed in the magnetized plasmas.

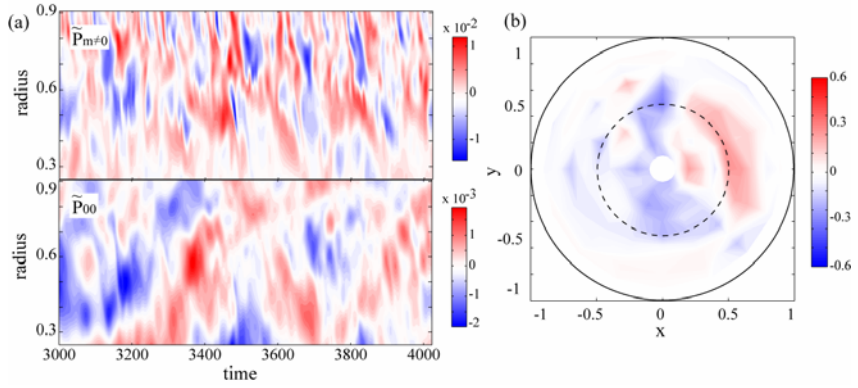

Fig. 2 (a) Time evolutions of the radial profiles of the electrostatic potential at $\theta = 0$ and $\zeta = 0$. The sum of the fluctuations without that of the (0,0) mode $\tilde{P}_{m\neq0}$ and the fluctuations of the (0,0) mode $\tilde{P}_{00}$ are shown. (b) 2-D profile of the correlation of $\tilde{P}_{m\neq0}$ at $\zeta = 0$ with $\tilde{P}_{00}$ at r/a = 0.5 (indicated with a dashed line).

4.2. two-dimensional imaging

Numerical diagnostics simulating turbulence diagnostics in experiments are carried out on the time series data [6]. Here, we show the 2-D imaging of the density fluctuation, taking account of the integral effect along the line of sight of the instruments. The BES observes line emissions from the injected neutral beam, which are related to the density. Detector arrays aligned two-dimensionally, as shown in Fig. 3 (a), give a 2-D image of density fluctuations. Numerical diagnostic gives the density integrated along the line of sight with the weight of the injected neutral beam intensity. Figure 3 (b) shows the snapshot of the density fluctuation profile. Compared with the local values at the points where the neutral beam intensity is the strongest on each line of sight (Fig. 3 (c)), it is found that the numerical diagnostic reproduces well the turbulence vortex shapes, though their outlines are blurred a little. In this case, the modes with low toroidal mode numbers are dominant, so the toroidal variation of fluctuations

is small, therefore, the numerical diagnostic represents the local values. From the obtained profile a trial to deduce $m = 0$ mode structure can be carried out by averaging interpolated data on a magnetic flux surface. The frequency spectrum from the deduced data along the dashed line in Fig. 3 (b) ($r / a = 0.5$) is shown in Fig. 3 (d). Compared with that of the (0,0) mode, there are higher frequency components. This is because the deduction is made in the vertically thin layer (6cm), so there remain finite m components. In this way, the simulation can be used to estimate how the reconstruction is matched or deviated from the actual feature.

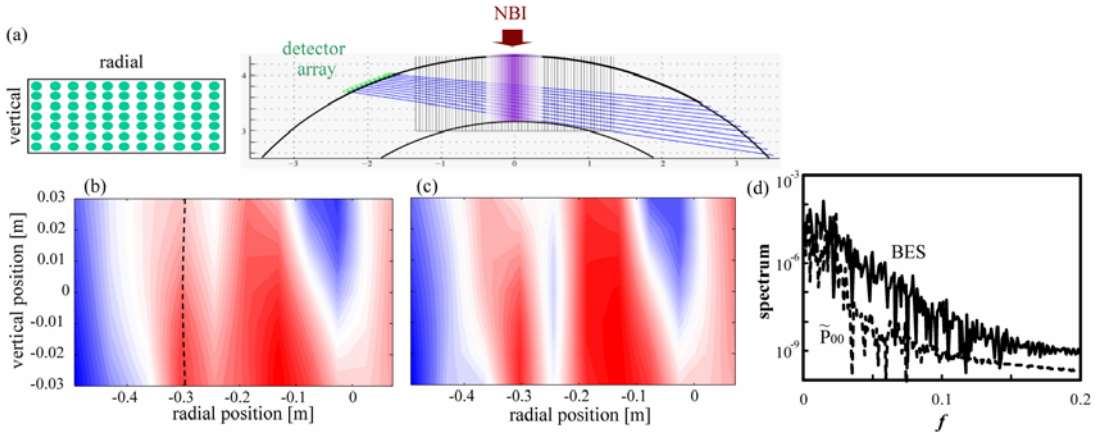

Fig. 3 (a) Schematic of the 2-D imaging of the density fluctuations. Snapshots of the 2-D image with (b) and without (c) the integral effect along the line of sights at t = 3000. (d) Frequency spectrum of m = 0 fluctuations deduced from the numerical BES signals (solid). The actual spectrum of the (0,0) mode is also shown (dashed).

5. Summary

The progress in the turbulence diagnostic simulator is presented by showing an example of data analyses with drift-interchange mode turbulence in helical plasmas. The multi-point spatial and temporal correlation analyses reveal the characteristic structures formed in the magnetized plasmas. The modules simulating experimental measurements subtract time series of fluctuations from the stored data, taking account of a finite spatial resolution of each instrument. The numerical diagnostics provide analyses as same in the experiments, which aid the development of the data analysis technique to deepen our physical understandings.

This work is supported by the Grant-in-Aid for Young Scientists (20760581) and for Scientific Research (21224014) of JSPS, by the collaboration program of NIFS (NIFS11KNST013) and of RIAM of Kyushu University.

References

[1] P. H. Diamond, *et al.*, Plasma Phys. Control. Fusion **47** (2005) R35
[2] A. Fujisawa, Nucl. Fusion **49** (2009) 013001
[3] N. Kasuya, *et al.*, Phys. Plasmas **15** (2008) 052302
[4] N. Kasuya, *et al.*, Plasma Fusion Res. **6** (2011) 1403002
[5] M., Wakatani, *Stellarator and Heliotron Devices* (Oxford University Press, Oxford 1998)
[6] N. Kasuya, *et al.*, Plasma Sci. Tech **13** (2011) 326